

# Directed follow-up strategy of low-cadence photometric surveys in Search of Transiting Exoplanets - II. application to *Gaia*

Yifat Dzigan<sup>1\*</sup> and Shay Zucker<sup>1†</sup>

<sup>1</sup>*Department of Geophysics, Atmospheric and Planetary Sciences, Tel Aviv University, Tel Aviv 69978, Israel*

## ABSTRACT

In a previous paper we presented the Directed Follow-Up (DFU) approach, which we suggested can be used to efficiently augment low-cadence photometric surveys in a way that will optimize the chances to detect transiting exoplanets. In this paper we present preliminary tests of applying the DFU approach to the future ESA space mission *Gaia*. We demonstrate the strategy application to *Gaia* photometry through a few simulated cases of known transiting planets, using *Gaia* expected performance and current design. We show that despite the low cadence observations DFU, when tailored for *Gaia*'s scanning law, can facilitate detection of transiting planets with ground-based observations, even during the lifetime of the mission. We conclude that *Gaia* photometry, although not optimized for transit detection, should not be ignored in the search of transiting planets. With a suitable ground-based follow-up network it can make an important contribution to this search.

**Key words:** methods: data analysis – methods: observational – methods: statistical – techniques: photometric – surveys – planetary systems.

## 1 INTRODUCTION

*Gaia* is a European Space Agency (ESA) mission, scheduled to be launched at 2013. It will provide astrometric, spectroscopic and photometric measurements of the sky between the 6th and 20th magnitude (Eyer et al. 2009). As the successor of *Hipparcos*, *Gaia* is supposed to improve on the accuracy of *Hipparcos*. Specifically in photometry, it is expected to reach a milli-magnitude (mmag) photometric precision down to the 16th *G*-magnitude (de Bruijne 2012). Nominally, this may enable the photometric detection of planetary transits (Dzigan & Zucker 2012).

According to our recent estimates (Dzigan & Zucker 2012), the potential yield of transiting planets from *Gaia* photometry can reach a few thousands transiting exoplanets, depending on the number of planetary transits that the telescope should sample to secure detection. Due to the low cadence of the observations, *Gaia* will typically sample very few transits, which implies the need for a detection algorithm that will be tailored for *Gaia* special features, and will require a minimal number of in-transit observations.

In a previous paper (Dzigan & Zucker 2011) we first presented a strategy, which we named Directed Follow-Up (DFU), that is suitable for the detection of transiting exoplanets in low-cadence surveys. DFU uses specially tailored ground-based follow-up observations to augment the low-cadence data. In this paper we use *Gaia* scanning law to simulate light curves of transiting planets, and ex-

amine the capability of our strategy to detect transits in *Gaia*'s photometry and to predict optimal timing of follow-up observation.

### 1.1 The *Gaia* mission

The primary goal of the *Gaia* space mission is to explore the formation, dynamical, chemical and star-formation evolution of the Milky Way galaxy. It will achieve those goals using high precision astrometry, that will be backed with photometry and spectroscopy. During its five-year run, *Gaia* will measure parallaxes, luminosities, and proper motions for  $\sim 10^9$  stars in our Galaxy and beyond, as well as quasars, Solar System objects and other galaxies (Lindegren 2010).

*Gaia* will operate in a Lissajous-type orbit, around the Sun–Earth L2 point, so it will corotate with Earth in its orbit around the Sun, at a distance of about 1.5 million kilometers from Earth, in the anti-Sun direction. The mission will have a dual telescope, with a common structure and common focal plane. The spacecraft will rotate around an axis that will be perpendicular to the two fields of view, with a constant rate of  $1^\circ$  per minute, in order to repeat the observations in the two fields of view. Due to the basic angle of  $106.5^\circ$  that will separate the astrometric fields of view on the sky, objects will transit the two fields with a delay of 106.5 minutes (de Bruijne 2012). The spacecraft's spin motion of six-hour period, and a 63-day-period precession will cause *Gaia* scanning law to be peculiar and irregular. This special scanning law will result in an average of 70 measurements per object.

*Gaia* will provide photometry in several passbands. The *BP*

\* E-mail: yifatdzigan@gmail.com

† E-mail: shayz@post.tau.ac.il

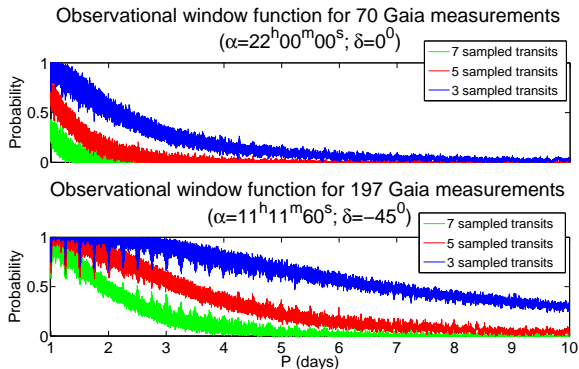


**Figure 1.** Observational window functions for two areas of *Gaia*'s sky. *Top*: A sky direction that *Gaia* is expected to visit 70 times, which is the average number of *Gaia* measurements over the five year time span of the mission. A similar window function was presented in Dzigan & Zucker (2012). *Bottom*: A sky direction that *Gaia* is expected to sample 197 times. Both window functions were calculated for a transit duration of 2 hr, for a minimum of three, five and seven in-transit observations.

(330–680 nm) and *RP* (640–1050 nm) bands correspond to the blue and red *Gaia* photometers. Those photometers will provide low-resolution spectrophotometric measurements. A third passband will be a wide and 'white' passband dubbed *G*, that will be centred on  $\lambda_0 = 673$  nm, with a width of  $\Delta\lambda = 440$  nm. One can expect a mmag precision in the *G* band, down to the 14th–16th *G* magnitude, and 10 mmag for the faintest objects (Jordi et al. 2010). The exact limiting magnitude for a 1 mmag precision depends on the final observing strategy and on instrumental factors, which are not yet fully determined (de Bruijne 2012).

Estimates of the expected yield of transiting planets from *Gaia* photometry range from hundreds to thousands (e.g., Høg 2002; Robichon 2002). In our previous paper (Dzigan & Zucker 2012) we estimated the expected yield, based on a statistical methodology, presented by Beatty & Gaudi (2008). We used assumptions regarding the galactic structure, effects of stellar variability, and transiting planet frequencies based on complete transit surveys (namely OGLE). As could be expected, our results suggested that *Gaia*'s transiting planet yield will depend strongly on the transit sampling (number of distinct transits that the telescope will sample per system). This intuitive result can be quantified by the observational window function (von Braun, Kane & Ciardi 2009), which is a function of the planet orbital period.

Assuming the existence of a transiting planet, the probability to sample a minimum of three, five and seven transits for a typical *Gaia* star, with 70 measurements, is shown in the upper panel of Fig. 1, together with another case, less probable, with 197 measurements, in the bottom panel.

The sharp minima and maxima in the window function for the extreme case are due to the six-hour-period spin of the telescope (Eyer & Migard 2005). For the case of a typical *Gaia* light curve with  $\sim 70$  measurements, if we assume the existence of a transiting Hot Jupiter (HJ), the probability to sample at least seven separate transits is practically negligible. The probability to sample a minimum of five transits is  $\sim 5$  per cent, but the probability to sample a minimum of three transits increases to  $\sim 30$  per cent. Thus, it may prove very beneficial to somehow relax the requirement for a minimum number of sampled transits. The DFU strategy aims to achieve exactly that.

## 1.2 Directed Follow-Up

The DFU strategy is based, in principle, on Bayesian inference, (e.g., implemented by a Markov-Chain Monte-Carlo – MCMC – procedure), that we use to estimate the posterior probability density functions of the transit parameters. We assume that a simple box-shape transit light-curve model describes the data (e.g. Kovács, Zucker & Mazeh 2002). This model involves five parameters: the period –  $P$ , phase –  $T_c$ , and width of the transit –  $w$ , and the flux levels in-transit and ex-transit. The MCMC procedure we chose to use was the Metropolis-Hastings (MH) algorithm (Dzigan & Zucker 2011).

We first apply the MH algorithm to the measurements of a target star. The results (after excluding the appropriate 'burning time') are Markov chains of the successful iterations, for each of the model parameters. From each chain we extract the stationary distribution of the parameter, which we use as the estimated Bayesian posterior distribution (Gregory 2005). If the low-cadence data happen to sample enough separate planetary transits, with sufficient precision, we expect the distributions to concentrate around the actual values of the parameters. Otherwise, If the data samples a small number of transits, the distributions will probably spread over different solutions, besides the unknown actual one.

The second step of the strategy is assigning to each point in time the probability that a transit will occur at that time. We calculate the transit probability using the posterior distributions found by the MH algorithm. For each point in time, we count the number of successful iterations whose values of  $P$ ,  $T_c$  and  $w$  predict that a transit will occur at the examined time. This results in a function we termed the Instantaneous Transit Probability – ITP.

An important part of the DFU strategy is the choice of stars to follow. We propose to choose stars for follow-up observations according to three criteria:

The first criterion follows from our observation that the most robust indication that a periodic transit-like signal exists in the data is the maximum value of the ITP. This should be intuitive if one remembers that by definition the ITP peak values actually represent the probability to sample a transit in follow-up observations.

The second criterion we propose is the skewness of the ITP, defined as

$$S = \frac{\langle (x - \langle \hat{x} \rangle)^3 \rangle}{\sigma^3}, \quad (1)$$

where  $x$  represents the ITP function values, and  $\langle \cdot \rangle$  denotes the averaging operation. In a sense, the skewness measures the amount of outliers in the ITP function, where 'outliers' refers here to ITP prominently high values. The relative absence of outliers, i.e., a 'flat' ITP, will yield a skewness that is close to zero ( $S = 0$  for a Gaussian distribution), which means that no time is preferred for follow-up observations.

The third criterion we propose is the Wald statistic of the transit depth posterior distribution. This simply quantifies the significance of the transit depth by measuring it in terms of its own standard deviation. Our experience shows that in case the algorithm explores the transit depth parameter space without converging, it might yield a high Wald statistic value, which we might erroneously interpret as evidence of a transit signal. Therefore, we propose to use this criterion only for prioritizing stars that have passed the first two criteria.

The third and final step of the strategy is to actually perform follow-up observations, at the times preferred by the ITP, thus optimizing the chances to detect the transit in a few observations as

possible. We then propose to combine both the ‘old’ data from the survey and the new observations, to recalculate the new posterior distributions that reflect our new state of knowledge, and to propose new times for the next follow-up observations.

In the most favorable case, where a follow-up observation happens to actually take place during transit, it will usually eliminate most spurious peaks in the period posterior distribution (PPD), except for the actual orbital period of the planet. Then a careful high-cadence photometric or spectroscopic follow-up of the candidates can confirm their planetary nature. In case we do *not* observe the transit in the follow-up observations, the new data will also eliminate some periods that will not fit our new state of knowledge, once again, resulting in new posterior distributions of the model parameters. The whole procedure should be repeated until the detection of a transiting planet, or, alternatively the exclusion of its existence (to a specified degree of certainty).

## 2 DFU FOR GAIA

We propose to apply the DFU strategy to the *Gaia* data in the following way:

1. Select the initial targets.
2. Run the MH algorithm for the targets that were selected in step 1.
3. Compute the Instantaneous Transit Probability function.
4. Prioritize stars for directed follow-up observations according to the ITP peak value and skewness.
5. Perform follow-up observations of the selected stars, and then combine the new data with *Gaia*’s data to repeat the process, starting from step 2.

In the first stage, when selecting the targets, one can obviously use various astrophysical criteria, e.g., the metallicity, which might affect the a priori probability of the star to host planets. This step can use the whole *Gaia* dataset with its various components of astrometric and spectroscopic information. Using the astrophysical and astronomical considerations, one will probably also eliminate beforehand eclipsing binaries, known variable stars, and non-main-sequence stars. We also propose to run a test for the possible presence of a transit signal in the data, by examining the statistical distribution of the light-curve values. Ideally, those values will have a bimodal asymmetric distribution, whose two peaks correspond to the in-transit and ex-transit levels, with corresponding relative probabilities. The plausibility of this distribution may serve as a preliminary screening tool, before applying the computationally demanding MH algorithm.

Once one has selected the targets and applied the MH algorithm to the light curves of the chosen targets, DFU can culminate in detection through one of three possible scenarios. The *first scenario* is a detection of the transit using solely *Gaia* photometry. We define detection as a case in which the MH algorithm results in a PPD that is centred around a single solution, (and maybe its harmonics and sub-harmonics). This very narrow distribution will ensure that the resulting ITP peaks will coincide with actual transits, with high detection probability, and that we will be able to use those preferred times to conduct high cadence follow-up observations, to confirm the transit nature of the periodic signal and refine its parameters.

Due to *Gaia*’s low cadence, and relatively small number of observations per star, in most realistic cases we expect to obtain posterior distributions that will exhibit several possible periods

(Dzigan & Zucker 2011). This will result in the other two more probable scenarios:

If the PPD exhibits a small number of peaks (that are not harmonics of each other), we will face the *second scenario*, in which a single follow-up observation will be needed in order to finally detect the transit. In the *third scenario*, the PPD will be distributed over many peaks, which means it will require more than a single follow-up observation in order to finally detect the transit.

## 3 SIMULATIONS

We simulated light curves of planetary transits according to *Gaia*’s scanning law and expected photometric precision, as of August 2011. We used the same scanning law setup as in Dzigan & Zucker (2012) to assign each planet with the timing sequence of *Gaia* observations, according to its location on the sky. Note that the details of the scanning law simulations depends on some arbitrary factors, depending on the exact timing of the mission, which is obviously not determined yet. The number of *Gaia* FOV crossings of a given object as a function of location in the sky, is influenced by the phasing of the scanning law we choose, thus our implementation of the scanning law is only representative, and specific attempts of transit detection and follow-up should be made using the actual timing of *Gaia* measurements.

Following Dzigan & Zucker (2012) we assumed one in-transit measurement per transit, for all the simulations we present in this paper. It is possible that a transit duration of a few hours will result in more than a single FOV crossing per transit, however, several in-transit measurements of the same transit do not have significant contribution for constraining the PPD. They can, however, be useful for eliminating calibration errors.

We simulated the errors as purely Gaussian. In order to test our strategy, we examined simulations of known transiting planets with orbital periods ranging from  $\sim 1$  to  $\sim 9$  days.

The simulations were assigned with different numbers of in-transit observations, by varying the transit phase, and with a range of transit depths ( $d = 0.01 - 0.001$  mag) to simulate different planetary sizes. Thus, we used the known period and duration ( $w$ ) of each planet, while varying the phase and depth, according to the case we aimed to test. Table 1 presents the orbital elements of the known exoplanets we used in the simulations.

In the upper panel of Fig. 2 we present an example of a simulated *Gaia* light curve of a transit with depth of 8 mmag, to illustrate the challenge to detect planetary transit in low-cadence photometric surveys. In the middle panel of Fig. 2 we show the same light curve, folded according to the transit phase, and in the bottom panel a light curve of the same star, with no transit signal.

In some cases, those that demonstrate the second and third detection scenario, we also simulated the directed follow-up observations, obtained on times that were indicated optimal for follow-up based on the ITP values. Each simulated follow-up observing sequence comprised four single exposures, two that were scheduled to occur within the ITP peak, and two before and after the peak. This was meant in order to sample times in and out of the suspected transit. We assumed a photometric error of 1 mmag.

Besides testing the detection using the full simulation of *Gaia*’s scanning law, we also addressed two additional issues. The first is detection based on only part of *Gaia*’s full mission lifetime. Wyrzykowski & Hodgkin (2012) described the *Gaia* Science Alerts team, that is assigned to handle mainly transient phenomena in the *Gaia* data stream. Supernovae, microlensing events, and

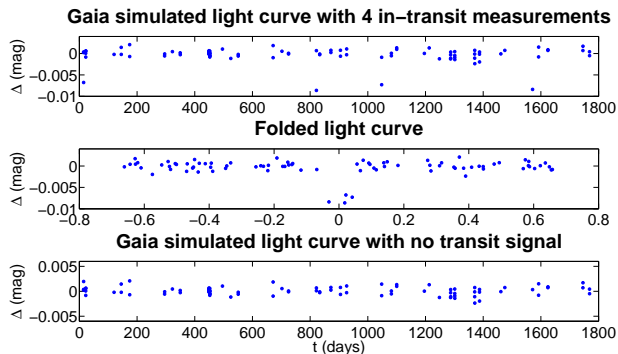


**Figure 2.** *Top:* Simulated *Gaia* light curve of WASP-4b, that corresponds to a transit depth of 8 mmag, and four in-transit measurements. *Middle:* The simulated light curve of WASP-4b, folded according to the transit phase. *Bottom:* Simulated light curve of the same star, but with no transit signal.

m-dwarf flares are just a few examples of the possible triggers that the team will study. Our DFU strategy may benefit from a similar follow-up network that will be able to follow-up on prominent ITP peaks during the mission lifetime. To test the value of such an effort we tested our strategy when only half of *Gaia* time span was used.

The second issue is the false-alarm rate. As we have shown in our previous paper (Dzigan & Zucker 2012), the false-alarm rate due to *Gaia*'s white Gaussian noise is negligible. However, McQuillan et al. (2012) estimated that more than 60 per-cent of the stars exhibit microvariability that is larger than that of the Sun. Due to *Gaia*'s low cadence, the effect of the stellar red noise (McQuillan et al. 2012) is simply an increase in the white noise level by 1 – 2 mmag. We therefore simulated thousands of *Gaia* light curves with increased Gaussian errors, and examined the false alarm rate due to stellar variability.

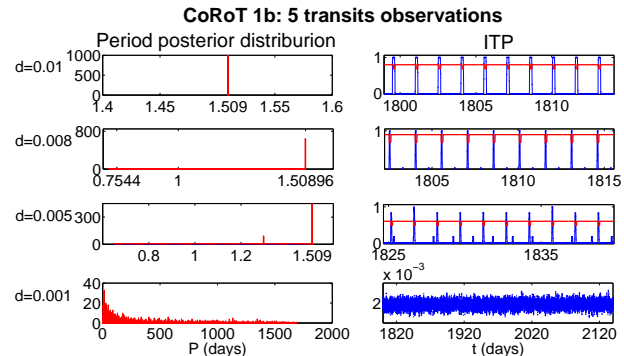
## 4 RESULTS

Table 2 presents a summary of the test cases we simulated and the simulation results. The first column is the name of the planet on which we based the simulation (sky location, period and transit duration). In some cases, the simulation included also the directed follow-up observing sequences, which is indicated in the relevant lines.

The second column is the total number of samples  $N_{\text{tot}}$ , which is determined by the planet coordinates through *Gaia*'s scanning law. In cases where we tested detection using half of the mission lifetime, the number is especially low. Next is the number of in-transit measurements,  $N_{\text{tr}}$ , followed by the transit depth  $d$ . The results of the simulation are summarized by the following columns which are the posterior mean transit depth  $\langle d \rangle$ , the Wald statistic  $W$ , the ITP maximum value and the ITP skewness  $S$ .

One immediate result that the table demonstrates is that a transit depth of 1 mmag is simply undetectable. All the detection criteria, the Wald statistic, the maximum ITP, and the ITP skewness, are practically similar to what we see when we simulate pure Gaussian noise. In the deeper transits,  $S$  is always larger than 1, which we chose as the threshold value for our second criterion.

Below we demonstrate the different detection scenarios we have mentioned. For each example (Fig. 3–6) we present the PPD and the ITP for various transit depths. We also show some simulations of directed follow up observations.



**Figure 3.** PPDs (left panels), and ITP functions (right panels) for the simulation of CoRoT-1b with five transit observations, for a range of transit depths.

### 4.1 First detection scenario

We used the planet CoRoT-1b to base on it the first-scenario simulations, where detection is possible based on *Gaia* data alone. Fig. 3 shows the PPD and the ITP we obtained. The choice of the simulated transit phase in such a way that five transits are sampled allows the detection. We see that for transits deeper than  $d = 0.005$  mag (The upper two panels), the PPDs are centred around a single distinct period, consistent with the known simulated period. As a result, the ITP prominent peaks coincide with the future transits of the planet.

We do not consider the case with a depth of 5 mmag (the third panel), an example of the first scenario, since a small secondary peak does occur in the PPD, which therefore renders it a second scenario case.

The figure also shows in the bottom panel the case of an undetectable 1 mmag transit. The difference in the PPD and the ITP is obvious.

### 4.2 Second detection scenario

We used CoRoT-4b to demonstrate the second scenario. We chose a transit phase that would imply sampling of three separate transits, although it is not very likely for such a long period planet ( $P > 9$  d). Fig. 4 shows the three cases, together with an undetectable 1 mmag transit. Clearly, the period distributions have two or three preferred periods, that are not harmonics of each other. That constitutes a second scenario case. In these cases, the most significant peaks of the ITP do coincide with the planetary transits, so the first follow-up observation that would have used the directed follow-up strategy, would detect it. Again, the bottom panel in the figure, shows, for comparison, a non-detection of the 1 mmag transit.

### 4.3 Third detection scenario

The planet WASP-4b serves as the base for our third-scenario simulations, where we chose a transit phase to sample four separate transits. Fig. 5 shows the results of the simulations with the four different transit depths we tried. The upper panel with a transit depth of 0.01 mag, is a clear example of the first scenario, while the lower panel, with a depth of 1 mmag, is a clear example of non-detection. In the two middle panels one sees that the period posterior distribution is multimodal.

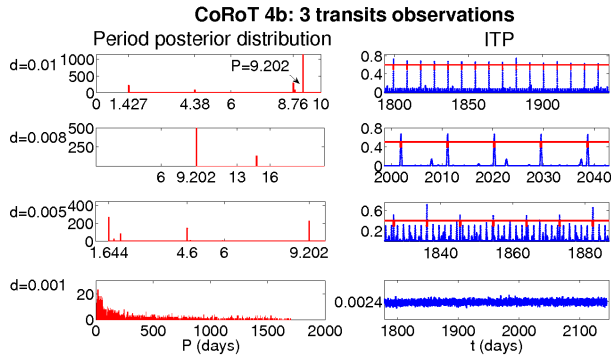


**Figure 4.** PPDs (left panels), and ITP functions (right panels) for the simulation of CoRoT-4b with three transit observations, for a range of transit depths.

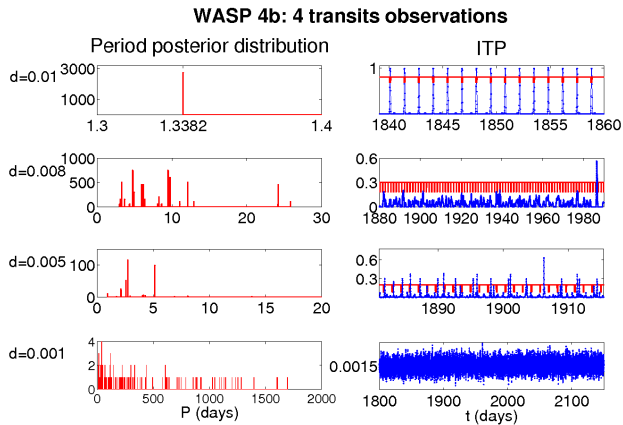


**Figure 5.** PPDs (left panels), and ITP functions (right panels) for the simulation of WASP-4b with four transit observations, for a range of transit depths.

The most prominent peaks of the resulting ITP functions do not coincide with the actual mid-transit times. However, according to the prioritization criteria (whose values are summarized in Table 2), the star would have been prioritized for follow-up observations. Combined with the low-cadence data, the follow-up should eliminate some of the wrong periods, allowing others to emerge, and eventually may lead to a detection.

We demonstrate the effect of the directed follow-up on the shallower case, where  $d = 5$  mmag. The result is depicted in Fig. 6. The upper panel shows that the first follow-up observing sequence, during the time of the highest ITP value, happens to occur not during a transit. However, the PPD resulting from combining the follow-up observations and *Gaia* data, modifies the distribution, as is shown in the middle panel, together with a new suggestion for a follow-up time. A look at the corresponding line in Table 2 shows the improvement in the prioritization criteria values. The next follow-up sequence, in the bottom panel, already shows the detection.

#### 4.4 Mid-lifetime

As we have shown in Dzigan & Zucker (2011), as time goes by, the ability to use the ITP to schedule follow-up observations degrades.

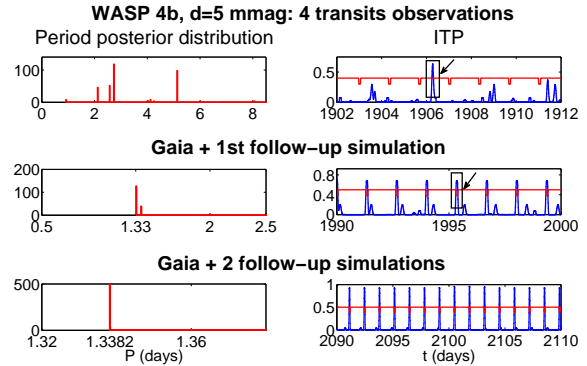


**Figure 6.** *Top:* PPD and ITP for the *Gaia* simulation of WASP-4b, with a depth of 5 mmag and four sampled transits. *Middle:* New PPD and ITP after adding the first follow-up observing sequence, that was simulated according to the marked ITP peak, which do not coincide with mid transit time. *Bottom:* New PPD and ITP after adding a second follow-up sequence, that was simulated according to the marked ITP peak, which this time did sample a transit.

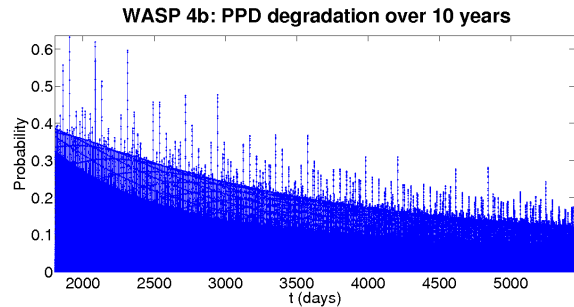


**Figure 7.** PPD degradation rate for ten years after *Gaia* will finish its operation, for simulation of WASP-4b, with transit depth of 5 mmag, and four in-transit datapoints.

We present an example of the ITP degradation rate for ten years past *Gaia* in Fig. 7. It is therefore crucial that the follow-up observations will take place as close as possible to the time the original low-cadence observations take place. In the case of *Gaia* it will probably be optimal to perform the follow-up while the mission still operates.

We show an example of this mid-lifetime follow-up detection using the known planet TrES-1b. We tailored the mid-transit phase so that the scanning law will sample four individual transits, during the full time span of the telescope. For a transit depth of 0.01 mag, the full mission lifetime yields a first-scenario detection, as the upper panels of Fig. 8 show. The ITP peak values are impressively close to 1.

We then continued by simulating only half of the mission lifetime, with the same transit phase, that implied only three observations during transit. According to Fig. 8, the deepest transit case,  $d = 0.01$  mag, results in two distinct peaks of the PPD, which are harmonics of a single one, indicating that this (mid-lifetime) case can be classified as a detection. The shallower transit cases yield more than three probable periods, and hence can be classified as third scenario cases.

The ITP values in this case are relatively high, and so is the

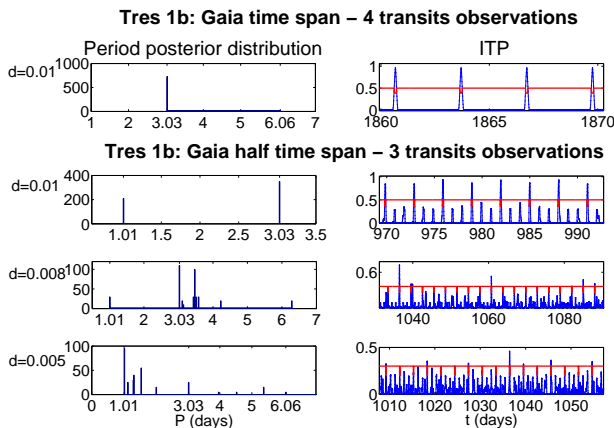


**Figure 8.** PPD and ITP for the full mission lifetime simulation of TrES-1b, and for half the mission lifetime.

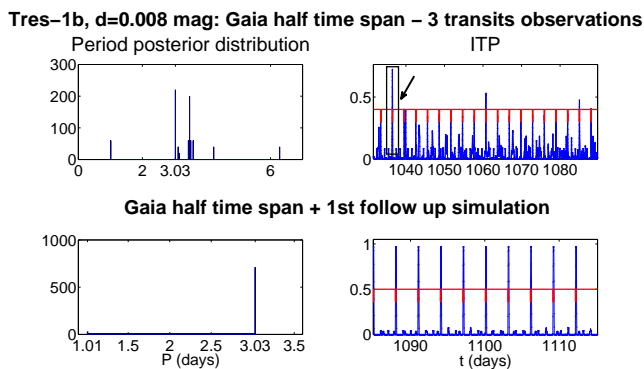


**Figure 9.** *Top:* PPD and ITP for the half lifetime simulation of TrES-1b with a depth of 8 mmag. *Bottom:* New PPD and ITP after combining the simulated follow-up observations (according to the marked ITP peak that coincide with mid transit) with *Gaia* data.

skewness, and we therefore conclude that there is a good chance that the DFU strategy will prioritize this object for follow-up, even after only half of the mission lifetime, as long as *Gaia* will sample at least three transits during this time.

We further simulated the follow-up observations in the case of  $d = 0.008$  mag. This single observing run was enough to exclude all the wrong periods, and allow a detection of the transiting planet, as the bottom panels of Fig. 9 show.

Based on numerous other simulations we performed of the half-lifetime span, we conclude that we will be able to trigger follow-up observations during *Gaia*’s lifetime, and in the cases where three transits will have been sampled in this interval, we may achieve detections in the second or third scenario.

#### 4.5 False alarms

We chose several values for the total number of measurements ( $N_{tot} = 60, 70, 90, 120,$  and  $180$ ) and simulated 1000 *Gaia* light curves for each  $N_{tot}$ , assuming white Gaussian noise of 2 – 3 mmag. We estimated the number of simulations that would have a transit-like dimming (a double-peak distribution of the magnitude, where the dimming would be in the range 0.005–

0.015 mmag), given the increased photometric error. We found that 28 simulations out of  $10^4$  pass this simple test.

However, our prioritization approach excluded all those cases, since they all had ITP skewness and peak values that were smaller than our chosen thresholds. The skewness values of the 28 false-positive cases ranged from 0.02 to 0.76 (three out of the 28 had skewness larger than 0.5), and their highest ITP peak values were much smaller than the 0.1 threshold, ranging from  $2 \times 10^{-3}$  to 0.013. It seems, therefore, that our prioritization scheme effectively eliminates those false detections.

On top of the outliers induced by white noise or stellar microvariability, calibration errors may also complicate the transit detection, as was examined by Tingley (2011). Once *Gaia* will operate, the calibration errors should be addressed and included in the DFU strategy, through the MCMC algorithm. In case “false” periods will be introduced to the PPD due to calibration errors, they should be eliminated by directed follow-up observations.

## 5 DISCUSSION AND CONCLUDING REMARKS

In this paper we examined the application of the DFU strategy, which we first introduced in Dzigan & Zucker (2011), to *Gaia* photometry. The DFU strategy can be used to prioritize stars for follow-up observations according to the probability to detect transiting planets around them. We presented here selected simulated scenarios, which represent a wider range of simulations we performed.

For all test light curves that we simulated with a transit depth larger than 1 mmag, we were able to use our approach to either recover the periodicity, or at least to propose times for directed follow-up observations that eventually led to detection. Furthermore, test light curves with no transit signal were never classified as candidates, and were not prioritized for follow-up observations.

For transits deeper than the typical HJ depth of 0.01 mag, in case *Gaia* will sample at least five individual transits, a secure detection will be possible based on *Gaia* data alone. If less transits are sampled by *Gaia*, the outcome of the MH algorithm will be a multimodal PPD. In these cases we found that we should be able to direct one or more follow-up observation that will be scheduled according to the ITP, that will allow us to detect the transit with minimal observational effort.

The limiting transit depth of the DFU approach, in the case of *Gaia*, seems to be around 1 mmag. Simulations with this depth were not prioritized for follow-up observations, and were indistinguishable from pure white noise.

Since MCMC methods are computationally demanding, we first propose to perform a simple test, in order to examine that a transit signal may exist in the data. Only then, after choosing the stars that pass this test, and after applying the appropriate astronomical considerations, we propose to explore the full parameter space using the MH algorithm and obtain the full posterior distributions. Once we run the algorithm on the selected stars, we can continue and prioritize them for follow-up observations according to the criteria we discussed in section 4.

The *Gaia* Photometric Science Alerts Team is responsible for generating alerts on anomalous events that will be detected in *Gaia* photometry. The facilities used by the team may also be used for follow-up observations, based on the DFU strategy. Alternatively, a dedicated follow-up network, suitable for observations of transiting planets (both high and low cadence) can complement *Gaia*’s observations, and be beneficial for transit detection.

We have noticed that the chances of detection depend directly

mainly on the number of sampled transits, and on the transit depth. Clearly, the number of sampled transits is a function of the total number of measurements, as we show in Fig. 1. Moreover, data points that do not sample a transit can exclude periods from the PPD, however, the in-transit measurements have the largest influence on the detection probability. This means that if, by chance, *Gaia* samples three individual transits for a certain object, before the end of the mission, we will be able to use this partial light curve, to trigger follow-up observations. Obviously, the probability to sample transits decreases as a function of decreasing number of measurements, and so the overall yield of planets from *Gaia* photometry will only be complete once the mission ends. Nevertheless, there is value in starting the DFU effort while the mission still operates. This may expedite the detection of transiting planets based on *Gaia* photometry.

As mentioned above, we found that even for a small transit depth, of the order of 5 mmag, we will usually be able to detect a planet with five sampled transits. In case *Gaia* samples less transits, the small transit depth can yield a detection in a follow-up campaign. The simulated case of WASP-4b with a 5 mmag transit, demonstrates the prospects of detecting Neptunian planets around late K-stars or around M-stars. The main problem with small transit depths is the difficulty to perform follow-up observations, but detections of such nature are well worth the observational effort.

To summarize, we believe we have demonstrated in this paper the feasibility of DFU for the case of *Gaia* photometry, and furthermore, its importance to fully exploit the extraordinary capabilities of the mission.

## REFERENCES

- Aigrain S. et al., 2008, A&A, 488, L43  
 Barge P. et al., 2008, A&A, 482, L17  
 Beatty T. G., Gaudi B. S., 2008, ApJ, 686, 1302  
 de Bruijne J. H. J., 2012, Ap&SS, 68  
 Dzigani Y., Zucker S., 2011, MNRAS, 415, 2513  
 Dzigani Y., Zucker S., 2012, ApJ, 753, L1  
 Eyser L., Mignard F., 2005, MNRAS, 361, 1136  
 Eyser L., Mowlavi N., Varadi M., Spano M., Lecoœur-Taïbi I., Clementini G., 2009, in SF2A-2009: Proceedings of the Annual meeting of the French Society of Astronomy and Astrophysics, eds., M. Heydari-Malayeri, C. Reyl  , & R. Samadi, p. 45  
 Gregory P. C., 2005, Bayesian Logical Data Analysis for the Physical Sciences: A Comparative Approach with ‘Mathematica’ Support, ed., Gregory, P. C., Cambridge University Press  
 H  g E., 2002, Ap&SS, 280, 139  
 Jordi, C., et al. 2010, A&A, 523, A48  
 Kov  cs G., Zucker S., Mazeh T., 2002, A&A, 391, 369  
 Lindegren L., 2010, IAU Symposium, 261, 296  
 McQuillan A., Aigrain S., Roberts S., 2012, A&A, 539, A137  
 Rietz S. et al., 2009, Astronomische Nachrichten, 330, 475  
 Robichon N., 2002, in EAS Publications Series, Vol. 2, EAS Publications Series, eds., O. Bienayme & C. Turon, p. 215  
 Tingley, B., 2011, A&AS, 529, A6  
 von Braun K., Kane S. R., Ciardi D. R., 2009, ApJ, 702, 779  
 Wilson D. M. et al., 2008, ApJ, 675, L113  
 Wyrzykowski L., Hodgkin S., 2012, New Horizons in Time-Domain Astronomy (IAU Symp. 285), eds. R. E. M. Griffin, R. J. Hanisch, & R. Seaman (Cambridge: Cambridge Univ. Press), 425

**Table 1.** Known planets used in the simulations

Planet Name	$P$ (days)	$w$ (days)	$d$ (mag)
CoRoT 1b <sup>1</sup>	1.5089557	0.1	0.025
CoRoT 4b <sup>2</sup>	9.20205	0.1583	0.013
TrES 1b <sup>3</sup>	3.0300722	0.104	0.022
WASP 4b <sup>4</sup>	1.3382282	0.0928	0.02

References:

1. Barge et al. (2008) 2. Aigrain et al. (2008) 3. Rätz et al. (2009) 4. Wilson et al. (2008)

**Table 2.** Summary of the simulation results

planet name	$N_{\text{tot}}$	$N_{\text{tr}}$	$d$	$\langle d \rangle$	$W$	Maximum ITP	$S$
CoRoT 1b	64	5	0.01	0.0099	70.9	1	2.5
CoRoT 1b	64	5	0.008	0.0081	205.2	1	4.88
CoRoT 1b	64	5	0.005	0.0051	44	1	4.16
CoRoT 1b	64	5	0.001	0.075	3.4	$2.1 \times 10^{-3}$	0.02
CoRoT 4b	63	3	0.01	0.0094	80.33	0.74	5.93
CoRoT 4b	63	3	0.008	0.0076	20.1	0.75	5.39
CoRoT 4b	63	3	0.005	0.0048	10.46	0.71	2.5
CoRoT 4b	63	3	0.001	0.08	2.2	$2.5 \times 10^{-3}$	0.08
WASP 4b	83	4	0.01	0.01	82.2	0.98	3.34
WASP 4b	83	4	0.008	0.0079	90.1	0.57	2.17
WASP 4b	83	4	0.005	0.005	79.2	0.63	3.5
WASP 4b	83	4	0.001	0.02	7.1	$1.9 \times 10^{-3}$	0.08
WASP 4b + 1st FU	83+4	4	0.005	0.005	180.4	0.7	2.86
WASP 4b + two FU	83+4+4	4+1	0.005	0.005	181.5	0.96	3.32
TrES 1b	98	4	0.01	0.01	19.6	0.97	4.5
TrES 1b	48	3	0.01	0.0098	83.4	0.94	3.1
TrES 1b	48	3	0.008	0.008	47	0.72	2.67
TrES 1b	48	3	0.005	0.0048	21.8	0.46	1.6
TrES 1b + 1st FU	48+4	3+1	0.008	0.0078	41.8	0.97	4.4